

CLAY MINERAL ANALYSES WITH THE CHEMCAM INSTRUMENT AT THE MARIMBA, QUELA AND SEBINA DRILL LOCATIONS, IN GALE CRATER, MARS. G. David<sup>1</sup>, A. Cousin<sup>1</sup>, O. Forni<sup>1</sup>, S. Schröder<sup>2</sup>, K. Rammelkamp<sup>2</sup>, R. Lévillé<sup>3</sup>, E. Gibbons<sup>3</sup>, N. H. Thomas<sup>4</sup>, P.-Y. Meslin<sup>1</sup>, E. Dehouck<sup>5</sup>, J. Lasue<sup>1</sup>, W. Rapin<sup>1</sup>, O. Gasnault<sup>1</sup>, R. C. Wiens<sup>6</sup>, N. L. Lanza<sup>6</sup>, S. Maurice<sup>1</sup>; <sup>1</sup>IRAP, Toulouse, France; <sup>2</sup>DLR, Institut für Optische Sensorsysteme, Berlin, Germany; <sup>3</sup>McGill, Montréal, Canada; <sup>4</sup>BlackSky, Seattle, WA, United States; <sup>5</sup>Univ Lyon, UCBL, ENSL, UJM, CNRS, LGL-TPE, F-69622, Villeurbanne, France; <sup>6</sup>LANL, Los Alamos, USA; [gael.david@irap.omp.eu]

**Introduction:** Since 2012, the Curiosity rover has been investigating the sedimentary rocks of Gale crater to constrain its past environments. The mineralogical and chemical characterization of alteration phases such as clay minerals is an important step to reach this objective. Among the payload of the rover, the CheMin X-ray diffraction instrument [1] identified clay minerals in most of the drill samples analyzed (up to ~30 wt.%) [2, 3].

The ChemCam Laser-Induced Breakdown Spectroscopy instrument [4, 5] onboard Curiosity provides a statistically significant survey of the chemistry of the rocks along the rover traverse. The submillimeter diameter of the laser beam (350-550  $\mu\text{m}$ ) enables it to probe fine features such as individual mineral grains. However, due to their small particle size and their mixture with igneous and other alteration products in Gale's rocks, direct detection of clay minerals by ChemCam is challenging.

The goal of this work is to assess the potential of ChemCam to detect clay minerals in bedrock composed of complex polyphase mixtures, using a combination of two geochemical markers: the LIBS hydrogen signal and the chemical index of alteration CIA [6]. First, we explored a limited laboratory dataset to determine the efficiency of these two criteria. Then, we analyzed the ChemCam data obtained at the Marimba, Quela and Sebina drill locations, to decipher the chemical composition of clay mineral(s).

**Geological setting:** Marimba and Quela are located in the Karasburg member of the Murray formation, and Sebina in the Sutton Island member. Drill samples analyzed by the CheMin instrument reveal that they contain respectively ~28 wt.%, ~16 wt.% and ~19 wt.% of phyllosilicates [2, 3]. Other crystalline minerals correspond to plagioclase (~21-31 wt.%), K-feldspar (~3 wt.%), pyroxene (~1-5 wt.%), quartz (~1-2 wt.%), hematite (~10-16 wt.%) and Ca-sulfates (~7-11 wt.%) with minor abundances ( $\leq 1$  wt.%) of halite and jarosite, in addition to an amorphous component (~40-52 wt.%). These samples show clay diffraction peaks consistent with the presence of Mg-rich trioctahedral and Fe-rich dioctahedral smectite resembling respectively saponite and

nontronite and/or Fe-montmorillonite [2]. The hydration of phyllosilicates is not fully constrained. CheMin data are consistent with the presence of collapsed smectite. However, the sample cells of the instrument are maintained at very low humidity that could promote loss of interlayer  $\text{H}_2\text{O}$  and collapse of clay mineral interlayers inside the instrument [7]. Here, we assume that a significant hydrogen content is carried by phyllosilicates (as supported by DAN results in the Glen Torridon member, [8]) although other mineral phases can be potential carriers (e.g., Ca-sulfates or amorphous materials).

**Methods:** In LIBS spectra, the H contents are estimated from an independent component analysis [9] expressed as ICA scores. In addition to hydration, we explored the chemical index of alteration (CIA, [6]). This index is intrinsically linked to smectite minerals as it is based on the ratio of the immobile element ( $\text{Al}_2\text{O}_3$ ) relative to mobile elements ( $\text{Na}_2\text{O}$ ,  $\text{CaO}$ , and  $\text{K}_2\text{O}$ ). It is defined as  $\text{Al}_2\text{O}_3/(\text{Al}_2\text{O}_3+\text{CaO}+\text{Na}_2\text{O}+\text{K}_2\text{O})\cdot 100$  (in molar abundances), and the increase of the CIA value above 50 (the plagioclase-K-feldspar join) is assumed to reflect the presence of clays since no other Al-rich phases were observed by CheMin.

**Laboratory observations:** First, we explored LIBS data obtained by [10] on mixtures of basalt with systematic variation in nontronite minerals NAu-1 and NAu-2. These two smectites are potential analogs of the clay minerals found in the Karasburg and Sutton Island members [11]. Laboratory samples were analyzed under martian environmental conditions with a ChemCam-analog instrument, and quantification was made with the same protocol as used for martian data, i.e., with the MOC quantification method [12]. In figure 1, we observe that these two criteria are well correlated with clay mineral abundances ( $R^2 > 0.92$ ). While not a universal proxy, we show that these two criteria combined could be successful to highlight the presence of clay minerals from the basaltic matrix in martian rocks, although the CIA values obtained on pure nontronite samples are only slightly above the CIA value expected for plagioclase and K-feldspar minerals (i.e.,  $\text{CIA}=50$ ).

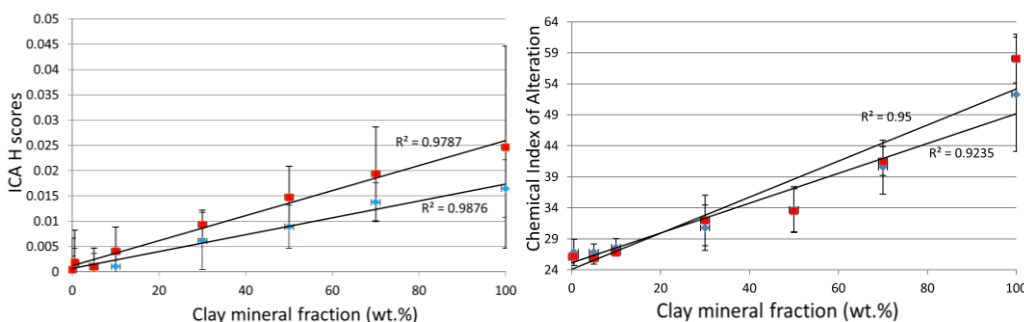


Figure 1: ICA H scores and CIA values as a function of clay mineral abundances from laboratory samples made of basaltic mixtures with two nontronites: NAu-1 (in red) and NAu-2 (in blue). LIBS data are taken from [10].

**Martian observations:** The ChemCam data used in this study included 1472 laser shots acquired on the same rock slabs as the Marimba, Quela and Sebina drill samples. Diagenetic features, soil targets and drill tailings were excluded from the dataset. Figure 2 shows the CIA values for each of the ChemCam shot-to-shot observations as a function of  $\text{Al}_2\text{O}_3$  and  $\text{MgO}+\text{FeO}_T$  abundances. ICA H scores are also represented in these plots with the color scale. In these diagrams, the chemical composition of mineral phases identified by CheMin from [2, 3] as well as the amorphous component (AmC) is represented. Different clay mineral candidates are also represented, to express potential trends expected in the ChemCam shot-to-shot data scatter. The compositions of nontronite (SWa-1), saponite (Griffith and SapCa-1), montmorillonite (STx-1, SAz-1, SWy-1), illite (IMt1/2) and interstratified illite-smectite (IScz-1) are provided by the Clay Minerals Society [13] and [14], and the NAu-1 and NAu-2 samples were analyzed in the laboratory.

In Figure 2, several mixing trends are visible on the shot-to-shot dispersion, indicating that ChemCam probed different mineral phases. A first trend is observed with high  $\text{Al}_2\text{O}_3$  abundance, low hydration and  $\text{CIA} \sim 50$ . This trend would be consistent with the contribution of andesine and/or sanidine minerals in the ChemCam analyses. A second trend toward low CIA and  $\text{Al}_2\text{O}_3$  (and  $\text{H}_2\text{O}$ ) abundances is consistent with Ca-sulfates and/or the bulk AmC compositions. In the  $\text{MgO}+\text{FeO}_T$  vs. CIA plot, trends consistent with these phases are also observed.

A third trend is observed that shows a low abundance of  $\text{Al}_2\text{O}_3$  but with a relatively high CIA value. Interestingly, ChemCam data forming this trend also recorded elevated hydration. Such features could be consistent with clay minerals. Among our clay candidates, nontronite (SWa-1 and NAU-1) or saponite (Griffith) could best explain the trend, whereas montmorillonite or illite seem to be too enriched in  $\text{Al}_2\text{O}_3$  content to be reasonable candidates. In the  $\text{MgO}+\text{FeO}_T$  vs. CIA plot, a trend towards high values seems to be also present, potentially rich in H although less obvious. Ferroan saponite (Griffith) is consistent with this trend or a mixture between saponite and nontronite (SWa-1 or NAU-1). Once again, illite and montmorillonite are not the best candidates to explain the observed trend.

**Conclusion:** In this study, we show that ChemCam could be able to reveal mixing trends in shot-to-shot data that are potentially related to the contribution of clay minerals. From CIA and hydrogen signals, two mineral mixtures with compositions trending toward ferroan saponite (Griffith) and nontronite (NAU-1 or SWa-1) could be present in the Marimba, Quela and Sebina drill locations in agreement with CheMin results [2, 3]. In this study, we highlight that hydration recorded by ChemCam in the sedimentary rocks of Gale could be associated with clay minerals although further work is needed to confirm this assumption. Indeed, the important caveat of this study lies in the unknown chemical composition and

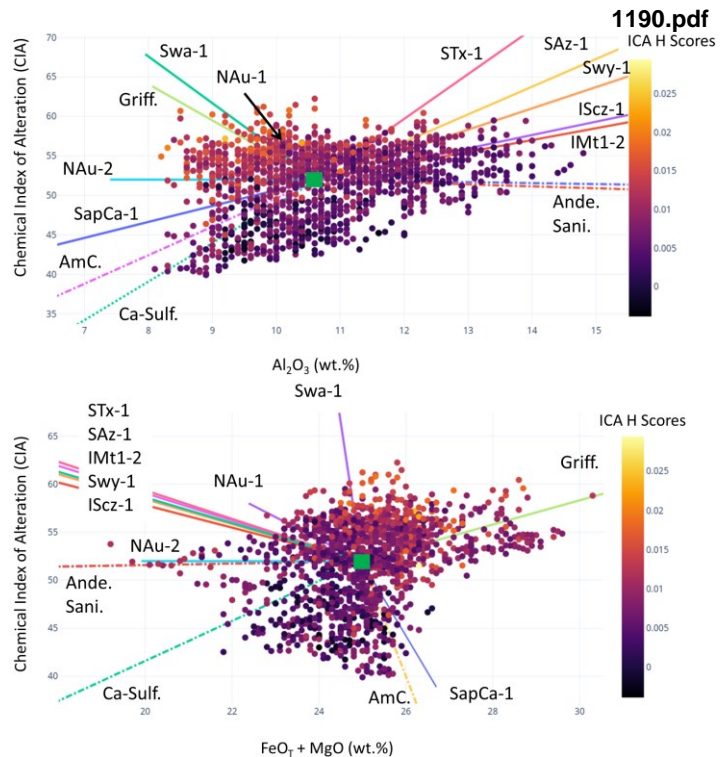


Figure 2:  $\text{MgO}+\text{FeO}_T$  and  $\text{Al}_2\text{O}_3$  abundances as a function of CIA values and ICA H scores for ChemCam LIBS data at the Marimba, Quela and Sebina drill locations. Average values are represented with the green squares. The compositions of clay mineral candidates are also represented to express potential trends in the shot-to-shot dispersion.

abundance of individual phases in the amorphous component that could be also responsible for the observed trends. Future work needs to be done on clay mineral signatures in ChemCam data (e.g., with minor and traces elements) to discard potential igneous and AmC surrogates and to confirm the good agreement between ChemCam and CheMin results. We have shown here that montmorillonite and illite compositions are not consistent with our observations, but additional clay mineral candidates should be explored including Fe-montmorillonite samples. Analyses in other Gale crater regions also need to be done to better constrain clay compositions. Such work would be particularly useful for the Glen Torridon region that contains elevated clay mineral contents according to CheMin results [15].

**References:** [1] Blake, D. et al., (2012). *Space Science Reviews*, 170(1), 341-399. [2] Bristow, T. F. et al., (2018). *Sci Adv*, 4(6). [3] Achilles, C.N., et al., (2020), *JGR: Planets*, 125(8). [4] Maurice, S. et al., (2012), *Space Science Reviews*, 170,95. [5] Wiens, R.C. et al., (2012), *Space Science Reviews*, 170, 167. [6] Nesbitt, H. W. et al., (1982). *Nature*, 299, 715-717. [7] Vaniman, D. T., et al., (2015) *AM. Mineral* 100 [8] Czamecki, S., et al., (2022). *This conference* [9] Forni, O. et al., (2013). *Spectrochimica Acta part B*, 86, 31-41. [10] Thomas, N. H. et al., (2018), *JGR: Planets*, 123(8). [11] Rampe, E. et al., (2021), *Geochemistry* 80(2). [12] Clegg, S. M., et al., (2017). *Spect. Acta. B*. [13] Olphena, H. V., & Fripiat, J. J. (2018). *Pergamon Press, Oxford*. [14] Treiman A. H. et al., (2014). *American Mineralogist*, 99, 2234-2250. [15] Bristow, T. F., et al., (2021). *Science*, 373(6551).